Supporting Information

Zhong et al. 10.1073/pnas.1423603112

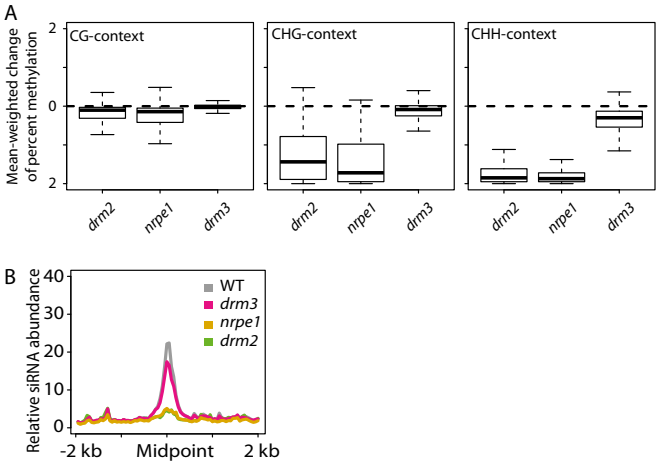

Fig. S1. Related to Fig. 1. DRM3 has moderate effects on DNA methylation and siRNA accumulation levels at RNA-directed DNA methylation targets. (*A*) Mean-weighted change [(% methylation in mutant − % methylation in WT/mean(% methylation in mutant, % methylation in WT)] in methylation at *drm2* CHH hypo-DMRs. In all three contexts, the reductions in methylation in *drm2* and *nrpe1* are more severe than *drm3* ($P < 2.2e{-}16$; Wilcoxon rank sum test). (*B*) Average levels of 24-nt siRNA over *drm2* CHH hypo-DMRs.

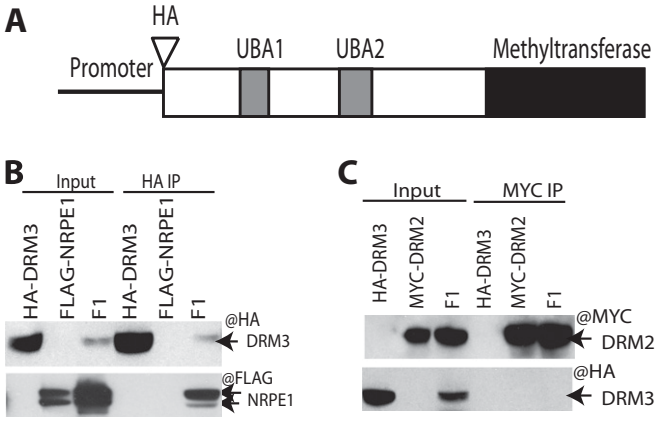

Fig. S2. Related to Fig. 3. DRM3 is associated with Pol V in vivo. (*A*) Schematic representation of domain structures of the epitope-tagged DRM3. (*B*) Coimmunoprecipitation assay confirming DRM3–NRPE1 interaction. (*C*) DRM3 doesn't interact with DRM2 by Co-IP.

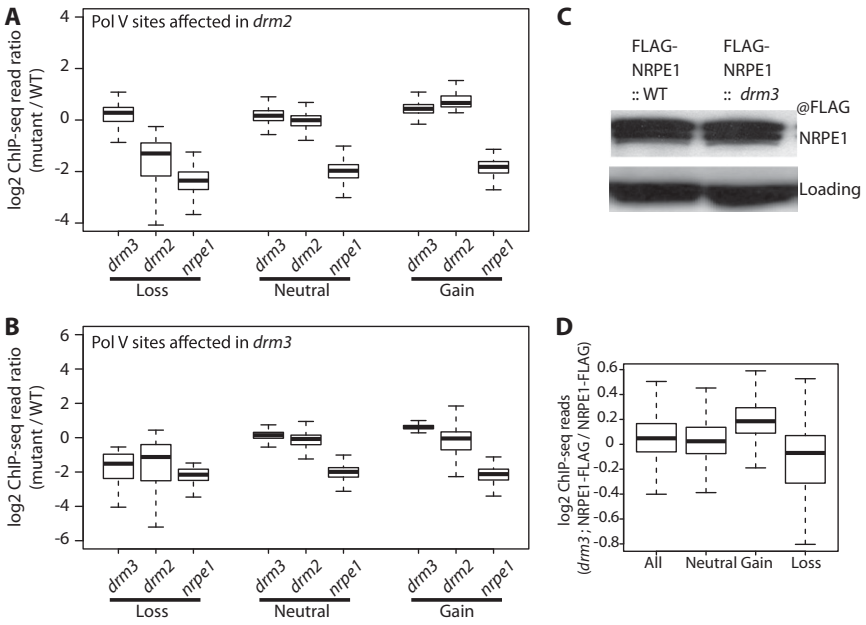

Fig. S3. Related to Fig. 4. Alteration of Pol V occupancy at defined binding sites in various mutants. (*A*) Ratio of ChIP-seq reads in various genotypes relative to WT at Pol V sites classified by the behavior of Pol V in *drm2* or (*B*) *drm3* ("Loss," "Neutral," or "Gain"). (*C*) Western blot detecting the NRPE1-FLAG protein levels in WT and a *drm3* mutant. (*D*) Ratio of ChIP-seq reads from an IP of NRPE1-FLAG in *drm3* compared with the NRPE1-FLAG IP in WT over all defined Pol V sites as well as Pol V sites classified by change of occupancy in a *drm3* mutant. "Gain" sites are significantly increased relative to "neutral" sites ($P < 2.2e{-}16$; Wilcoxon rank sum test). "Loss" sites are significantly decreased relative to "neutral" sites ($P = 3.211e{-}09$; Wilcoxon rank sum test).

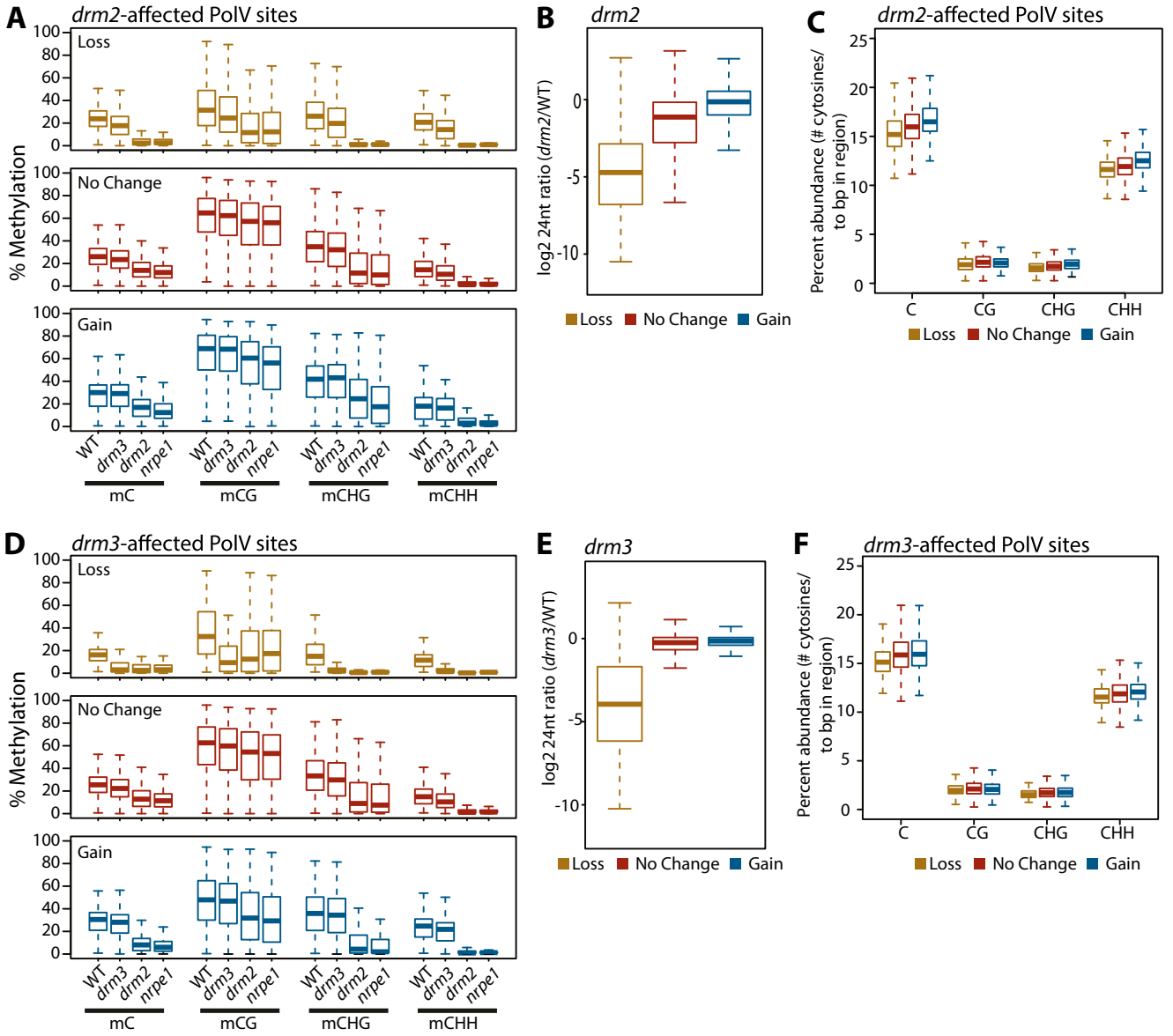

Fig. S4. Related to Fig. 5. Pol V association with chromatin in *drm* mutants is correlated with DNA methylation levels, siRNA levels, and cytosine contents at binding sites. (*A*) Methylation levels for different cytosine contexts at the loss, gain, or no change in *drm2* Pol V sites across multiple genotypes. Methylation levels for CG, CHG, and CHH are significantly lower at *drm2* loss sites compared with methylation levels at *drm2* neutral sites ($P < 2.2e{-}16$; Wilcoxon rank sum test). Overall methylcytosine levels are also lower at *drm2* loss sites compared with *drm2* neutral sites ($P = 2.276e{-}08$; Wilcoxon rank sum test). (*B*) The ratio of 24-nt sRNAs abundance of *drm2*/WT at Pol V sites classified by behavior in *drm2* ("Loss," "No Change," or "Gain"). "Loss" sites in *drm2* show a significantly greater decrease in siRNA levels than "No Change" sites ($P < 2.2e{-}16$; Wilcoxon rank sum test) whereas "Gain" sites show a smaller decrease than "No Change" sites ($P < 2.2e{-}16$; Wilcoxon rank sum test). (*C*) Percentage of cytosines found at Pol V sites classified by behavior in *drm2* ("Loss," "No Change," or "Gain"). Cytosine content in all three contexts (as well as total cytosine content) is significantly lower at *drm2* "Loss" sites compared with "No Change" sites ($P < 2.2e{-}16$ for C and CG sites, $P = 3.933e{-}13$ for CHG sites, and $P = 1.661e{-}09$ for CHH sites; Wilcoxon rank sum test). (*D*) Same as *A* except sites are classified based on change of Pol V occupancy in *drm3*. Methylation levels for C, CG, and CHG methylation are lower at drm3 loss sites compared with methylation levels at *drm3* neutral sites ($P < 2.2e{-}16$; Wilcoxon rank sum test). CHH methylcytosine levels are also lower at *drm3* loss sites compared with *drm2* neutral sites ($P = 1.034e{-}05$; Wilcoxon rank sum test). (*E*) Same as *B* except ratio of 24-nt sRNAs of drm3/WT at Pol V sites classified by behavior in *drm3*. "Loss" sites in *drm3* show a greater decrease in siRNA levels than "No Change" sites ($P < 2.2e{-}16$; Wilcoxon rank sum test) whereas "Gain" sites show a smaller decrease than "No Change" sites ($P = 5.604e{-}10$; Wilcoxon rank sum test). (*F*) Same as *C* except at Pol V sites classified by behavior in *drm3*. Cytosine content in all three contexts (as well as total cytosine content) is lower at *drm2* "Loss" sites compared with "No Change" sites ($P = 0.0003664$ for C site, $P = 0.09841$ for CG, $P = 0.0001914$ for CHG sites, and $P = 0.02756$ for CHH sites; Wilcoxon rank sum test).

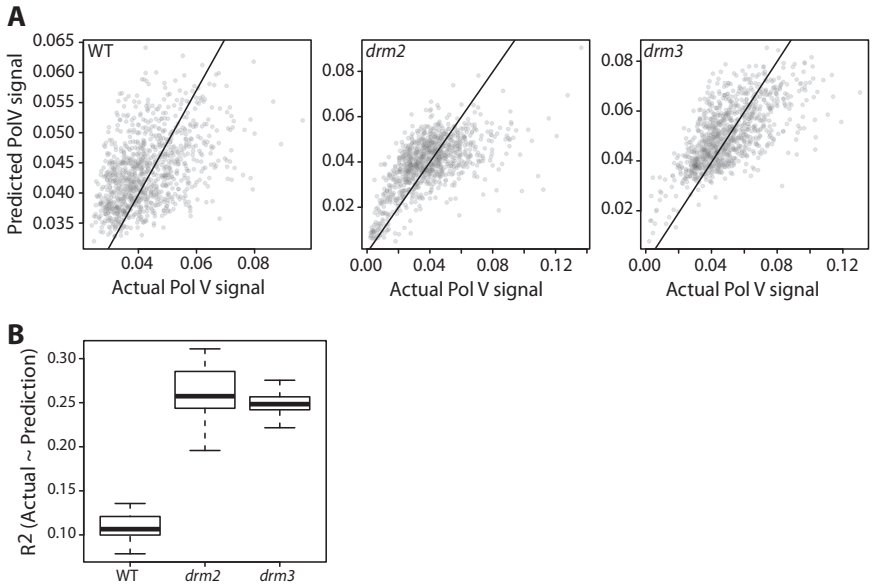

Fig. S5. Related to Fig. 5. Modeling Pol V behavior at defined sites in various genotypes. (*A*) Scatterplots of actual versus predicted Pol V ChIP-seq signal for the model with the median R^2 value from Fig. 5*C* for each genotype. (*B*) Same as Fig. 5*C* except distribution of R^2 values with models generated without mCHH or sRNA data. The WT R^2 values are significantly less than both the *drm2* and *drm3* values (P = 5.96e−08; Wilcoxon signed rank test).

Table S1. Listing of proteins identified in DRM3 purifications filtered at 10% of DRM3 (related to Fig. 3)

Protein	AGI code	Spectra	Unique peptides	% Coverage	NSAF	% DRM3
DRM3	At3g17310	94	17	33	922	100
	At2g27710	14	5	56	849	92
	At2g27720	13	5	56	788	85
	At3g47370	8	4	25	457	50
	At3g28500	6	4	34	364	39
	At4g32470	6	3	29	343	37
	At3g52580	7	4	24	325	35
NPRE3A	At2g15430	12	6	23	262	28
	At2g20450	5	3	25	260	28
	At5g53560	5	3	30	260	28
	At1g78380	8	3	15	254	27
	At5g25460	12	5	17	226	24
	At5g47030	6	5	30	206	22
NRPE9A	At3g16980	3	2	21	183	20
	At5g63310	6	3	13	181	20
	At4g14800	5	3	16	175	19
	At1g24360	8	3	14	174	19
	At1g54780	7	4	15	171	18
	At5g63570	11	6	21	162	17
	At3g49470	5	3	18	160	17
	At2g22230	5	3	16	158	17
NRPE7	At4g14660	4	4	32	157	17
NRPE3B	At2g15400	7	4	16	153	17
	At3g10060	5	3	20	151	16
	At5g13450	5	4	22	146	16
	At3g47470	5	3	19	138	15
	At5g67590	3	2	15	136	15
	At5g08530	9	5	13	129	14
	At4g01150	3	2	18	127	14
	At5g22580	2	2	22	125	14
NRPE11	At3g52090	2	2	17	120	13
NRPE2	At3g23780	20	13	14	119	13
	At2g24020	3	3	19	114	12
	At1g13280	4	2	11	109	12
	At3g06030	3	2	16	105	11
	At5g10160	3	3	14	95	10
	At1g78830	6	3	9	92	10
NRPE1	At2g40030	20	13	8	70	8

The percentage of DRM3 (% DRM3) column indicates the approximate stoichiometry of each copurifying protein as a function of the normalized spectral abundance factor (NSAF). Arabidopsis Genome Initiative (AGI) code uniquely defines a specific locus in the genome.

Table S2. Listing of proteins identified in NRPE1 purifications filtered at 0.2% of NRPE1 (related to Fig. 3)

Protein	AGI code	Spectra	Unique peptides	% Coverage	NSAF	% NRPE1
NRPE1	At2g40030	1,645	185	53	5,167	100
NPRE12	At5g41010	37	7	75	4,503	87
NRPE5	At3g57080	156	17	40	4,361	84
NPRE3A	At2g15430	210	31	62	4,086	79
NRPE11	At3g52090	73	12	73	3,906	76
NRPE3B	At2g15400	172	23	59	3,346	65
NRPE9A	At3g16980	61	11	60	3,321	64
NPRE9B	At4g16265	51	11	55	2,777	54
NRPE2	At3g23780	472	70	36	2,500	43
NRPE10	At1g11475	17	2	13	1,486	29
NRPE5-Like	At3g54490	50	9	32	1,332	26
	At1g72730	58	13	26	870	17
NRPE6A	At5g51940	18	7	51	776	15
NRPE4	At4g15950	19	3	16	737	14
NRPE7	At4g14660	19	6	36	663	13
	At1g55060	23	4	14	620	12
NRPE8A	At1g54250	6	3	27	255	5
	At5g52420	8	2	5	205	4
NRPE6B	At2g04630	4	4	35	172	3
	At3g10450	5	5	19	160	3
	At5g46930	2	2	25	148	3
AGO4	At2g27040	20	14	19	134	2.6
DMS3	At3g49250	8	6	20	118	2.3
	At1g07400	3	2	18	118	2.3
	At4g31490	14	10	13	91	1.7
	At4g38510	6	5	15	76	1.5
	At1g10200	2	2	7	65	1.2
	At3g55770	2	2	9	62	1.2
	At3g28715	3	3	13	53	1.0
	At3g61240	4	2	5	49	0.9
	At4g21800	3	2	7	49	0.9
	At5g56500	4	4	9	42	0.8
DRD1	At2g16390	5	5	8	35	0.7
	At4g35260	2	2	11	34	0.7
	At4g11380	4	4	5	28	0.5
DRM3	At3g17310	3	3	10	26	0.5
	At2g29370	3	3	6	22	0.4
	At4g31160	6	5	4	20	0.4
	At5g42220	2	2	3	14	0.3
SPT5L	At5g04290	3	3	3	13	0.2

The percentage of NRPE1 (% NRPE1) column indicates the approximate stoichiometry of each copurifying protein as a function of the normalized spectral abundance factor (NSAF).

Table S3. List of primers used in this study

	Primer numbers	Primer sequences from 5′ to 3′
DRM3	JP3477	GTCGACATCCTGATAGAATAGTTATATCTCAAGTTTATCACTGC
Cloning	JP3479	GTCGACATAACTTAAAACCTTATAATTAGATCAGATGTAAAACTTGTTCG
Actin	JP2452	TCGTGGTGGTGAGTTTGTTAC
	JP2453	CAGCATCATCACAAGCATCC
IGN22	JP9978	CGGGTCCTTGGACTCCTGAT
	JP9979	TCGTGACCGGAATAATTAAATGG
IGN6	JP6618	TTTCGCCGTCACTAACATGTAATG
	JP6619	GAAGTAGCTTTTTCGGTCCAGTTC
IGN5	JP6606	TCCCGAGAAGAGTAGAACAAATGCTAAAA
	JP6607	CTGAGGTATTCCATAGCCCCTGATCC
P7	JP10061	CGTTATGACAAAAACGATGACG
	JP10062	CATGTTATCTTTTGGAAAAAAATG
P8	JP10073	GAAAACAAAAGTTATACTTTG
	JP10074	GGTGTTTCATTCACTATCGTCC
P9	JP10075	CCGTTTCTGGGTAGGTCGGC
	JP10076	CCAATTCTTGACTGGAGTGGAC
P17	JP11893	TAACTTTGACCAACGCCAATG
	JP11894	AAATGACAATGTGGATGAAGTACAA
P18	JP11895	AATTGCAAGAGTTCTCGCTAAACA
	JP11896	GTTGTTAACGCTTCGGCCACTA
P19	JP11897	ACTAAGCCTCAACGGAACGGA
	JP11898	GGGGAAGCTTTGTGAGGGTTC